

# Empirical validation of a hyperspectral systems model for subpixel target detection using data from a new UAS field collection

Chase Cañas<sup>a</sup>, John P. Kerekes<sup>a</sup>, Emmett J. Ientilucci<sup>a</sup>, and Scott D. Brown<sup>a</sup>

<sup>a</sup>Rochester Institute of Technology, Center for Imaging Science, 1 Lomb Memorial Dr.,  
Rochester, NY 14623

## ABSTRACT

Systems modeling of hyperspectral instruments is effective for forecasting instrument performance of subpixel target detection. A new reconfiguration of the statistical model-based tool FASSP (Forecasting and Analysis of Spectroradiometric System Performance) is currently in development at the Rochester Institute of Technology, for purposes of exploring systems limitations in subpixel detection. To validate the baseline functioning of the statistical model, empirical analyses using real data were cross-examined with model predictions. The real data were collected from a field experiment using a hyperspectral sensor on-board an unmanned aerial system (UAS). To assist in model validation, a variety of novel subpixel targets, spanning a range of constant target percentages, were designed and deployed in the field. The UAS was advantageous in enabling the research team to maintain full end-to-end control of the system parameters within the experiment. This includes selecting specific flight lines, collecting ground truth spectral measurements, deploying specific targets, and processing raw data into geophysical units of surface reflectance. The study revealed close alignment between the empirical results and modeled predictions.

**Keywords:** target detection, hyperspectral, subpixel, UAV, CMOS, limitations

## 1. INTRODUCTION

### 1.1 Subpixel Target Detection with Hyperspectral Sensors

Hyperspectral sensors collect 3-dimensional data cubes, consisting of both spatial (2D) and spectral (1D) information. Spatial information can provide geometric context of an object, while spectral information can provide material context. In subpixel target detection, the spectral information is leveraged to identify materials from an object ‘smaller than a pixel’. In other words, an object can be spatially unresolved, however, the material is still identifiable using only its spectrum of radiation collected across *many* bands. For hyperspectral sensors, *many* bands implies there may be dozens, hundreds, or even thousands of contiguous wavelength regions, which characterizes the spectral resolution. Mathematically, the linear combination of a target and background spectra in a single mixed pixel can be defined as

$$\alpha\boldsymbol{\mu}_T + (1 - \alpha)\boldsymbol{\mu}_B \quad (1)$$

where  $\boldsymbol{\mu}_T$  is the target spectrum,  $\boldsymbol{\mu}_B$  is the background spectrum, and  $\alpha$  is the target percentage. The *smaller* the target percentage becomes, the *more* the background spectrum contaminates the mixed pixel, reducing the probability of detection of the target. With empirical data, an algorithm facilitates the detection of a target spectrum across every pixel in an image. Pixels without target spectra induce *clutter* in the detection process. To account for all these conditions, the algorithm typically utilizes a target reference spectrum,  $\boldsymbol{\mu}_T$ , background mean spectrum of the image,  $\boldsymbol{\mu}_{Bave}$ , and background covariance matrix of the image,  $\boldsymbol{\Sigma}_{Bave}$ . A visual interpretation of the features in subpixel target detection is shown in Fig. 1a.

---

Further author information: (Send correspondence to C.C.)

C.C.: E-mail: cc1903@rit.edu

## 1.2 New Location for UAS Data Collections

A 177 acre property was recently gifted to the Rochester Institute of Technology (RIT) to expand the research capabilities of the university. The site, referred to as the Tait Preserve of RIT, has been an important location by researchers in the Digital Remote Sensing Laboratory (DIRS) for conducting experiments with unmanned aerial system (UAS) instruments. The location is desirable given the diversity of the landscape, which includes a 60 acre lake, open fields, trees, and a variety of vegetative species. A recent collection in October of 2021 involved the deployment of novel targets for research in subpixel target detection. The general imaging acquisition system uses a 272 band hyperspectral sensor (Headwall Nano Hyperspec) mounted onto a lightweight UAV platform (DJI Matrice 600). Images of the sensor, imaging platform, and location where the target were deployed are shown in Fig. 1b.

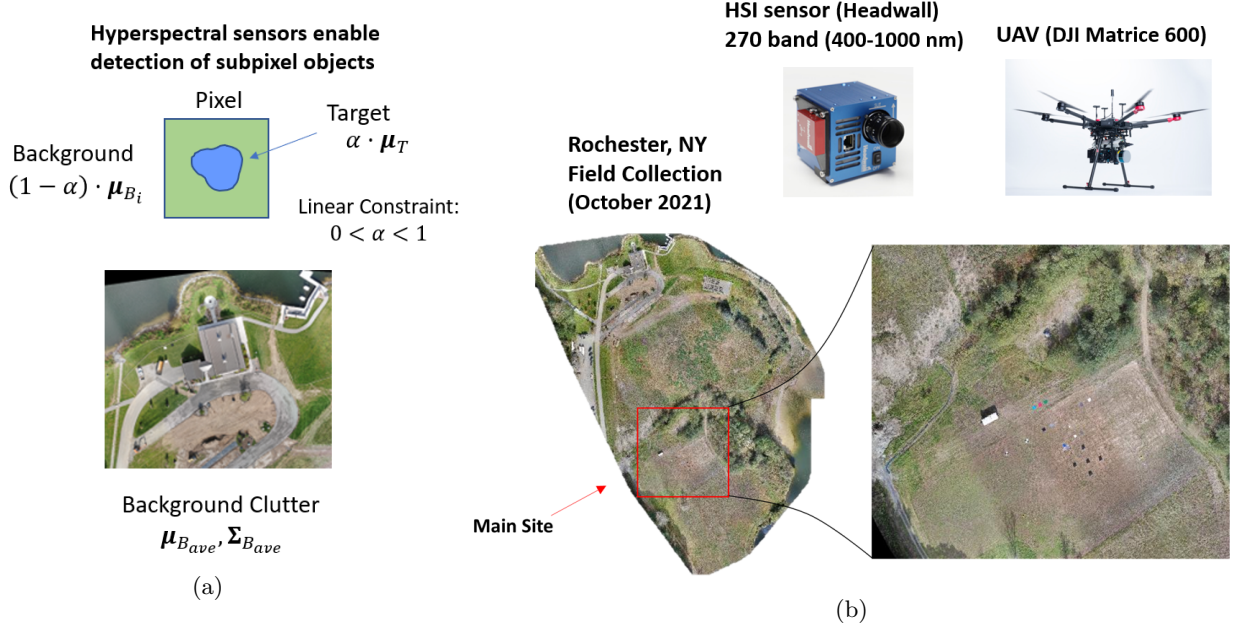


Figure 1: (a) Basic features of the subpixel target detection process, including the target reference spectrum,  $\mu_T$ , mixed pixel background spectrum,  $\mu_{B_i}$ , mean background spectrum of the image,  $\mu_{B_{ave}}$ , and background covariance matrix of the image,  $\Sigma_{B_{ave}}$ ; (b) Collection of images of the hyperspectral instrument, imaging platform, and field location where the experiments in subpixel target detection were performed.

## 2. METHODOLOGY

### 2.1 Systems Model for Subpixel Target Detection

Systems models are useful for forecasting performance and assessing limitations across various elements of the imaging chain. The imaging chain involves the process of how images are acquired, from the propagation of radiation of a material, through the absorption and scattering of atmospheric particles, to the digitization of electrons in the sensor. A systems model for subpixel target detection has been developed, referred to as the Forecasting and Analysis of Spectroradiometric System Performance (FASSP).<sup>1</sup> This is a statistical model for hyperspectral sensors, with a basic concept of propagating the 1st and 2nd order statistics (i.e. mean vector and covariance matrix) of the target and background materials through the imaging chain. After modeling the imaging chain, additional processing including atmospheric compensation (e.g. ELM) and feature selection (e.g. band selection, PCA) are applied to the transformed statistics. As a result, probabilities of detection and false alarms are generated to produce receiver operating characteristic (ROC) and various trade study curves (e.g. detection versus target percentage).

A new reconfiguration of the historical model (FASSP) is currently under development at RIT, with funding supported through the NGA University Research Initiative (NURI). The objective is to enhance the current capabilities of the model and provide a software tool to the community, for purposes of investigating fundamental limits of detection in hyperspectral imagers. To initiate the project, it was desirable to validate the model’s baseline functionality. Successful validation should instill confidence in the users’ ability to generate accurate predictions similar to real observations from empirical data. In addition, validation efforts are important for assessing sources of error or uncertainty, which provides valuable insight on the development of new improvements of the model framework during the re-design phase.

## 2.2 Novel Targets for Subpixel Experiments

Novel targets were designed, fabricated, and deployed in the recent October 2021 UAS collect for enhancing research in subpixel target detection. The basic concept involves targets consisting of constant percentages of target and background materials. This provided valuable insight, as historically it is extremely difficult to accurately ground truth the exact target percentage within a pixel due to a variety of factors. This includes pixel phasing, PSF blurring, geometric processing errors, noise, and spectral spatial misregistration errors. The targets were designed with various geometric structures for initial conceptual testing. Six targets, composed of birchwood material were sized approximately 12” x 12” and fabricated using a laser cutting machine. Three of targets were designed with a constant target percentage of 25%, but with varying geometric structures. The remaining three targets were designed with constant target percentages of 10%, 50%, and 75%. Lastly, four 12” x 12” birchwood targets with 100% target percentage were deployed for “full pixel” ground truth information of the birchwood material. The targets were used in the empirical validation of the hyperspectral systems model.

## 2.3 Model Parameters Based on Empirical Data

Table 1: Systems parameters defined in the hyperspectral model, characterized from the UAS Oct. 2021 data.

Scene		Atmosphere	
Target:	Birchwood	Solar Zenith Angle:	58°
Background in Subpixel:	Soil	Meteorological Range:	10 km
Scene Background:	Soil, Grass, Permaflect	Atmospheric Model:	Mid Latitude Summer
Scene Percentages:	49.2, 50.3, 0.5	Aerosol Model:	Rural Clear
Data Source:	UAS October 2021		
Sensor		Processing	
View Zenith Angle:	0° (nadir)	Algorithm:	Matched Filter
Bands:	270	Atmospheric Compensation:	ELM
Altitude:	119 m	Band Selection:	Entire Range (0.4-1.0 $\mu\text{m}$ )
Aperture:	4.8 mm		
IFOV:	0.3681 mrad		
nBits:	12		
Noise:	~14 e-		

To validate the hyperspectral model, a synthetic scene was generated using parameters derived from the October 2021 empirical data collection. The goal was to emulate the system parameters and performance observed in the empirical data within the systems model. An outline of the model parameters are shown in Table 1. The mixed pixels were modeled assuming a linear mixture of birchwood (target) and soil (background) materials. This was chosen given the subpixel targets in the real scene were deployed on primarily a soil background. The synthetic scene consisted of soil, grass and permaflect materials with fractions of 49.2%, 50.3% and 0.5%, respectively. These material were chosen given the diversity of their spectral signatures (i.e. shape and magnitude), such that the detection process was difficult but not overly complex. The fractions were determined

by calculating the number of target and background samples in the empirical dataset. The spectral libraries of these materials inputted into the model were generated using “full pixel” samples from the empirical image data. The atmospheric model parameters were best chosen to represent the actual conditions of the scene during data collection. The sensor model parameters were approximated using data sheets and lab measurements. During the processing stage of the model, a matched filter algorithm (mean centered and normalized) was applied to the mean vector and covariance matrices of the target and background materials. For more information regarding this process and the generation of detector output scores, refer to reference 1. Lastly, the target reference spectrum,  $\mu_T$ , in the detector algorithm was defined using the mean of “full pixel” samples across the center region of the birchwood material, for both empirical and model-based studies.

### 3. RESULTS

#### 3.1 Validation

Model validation was achieved through comparison of model and empirical results through various stages of the imaging and processing chains. Intermediate stages include atmospheric and sensor validation, as shown in Fig. 2.

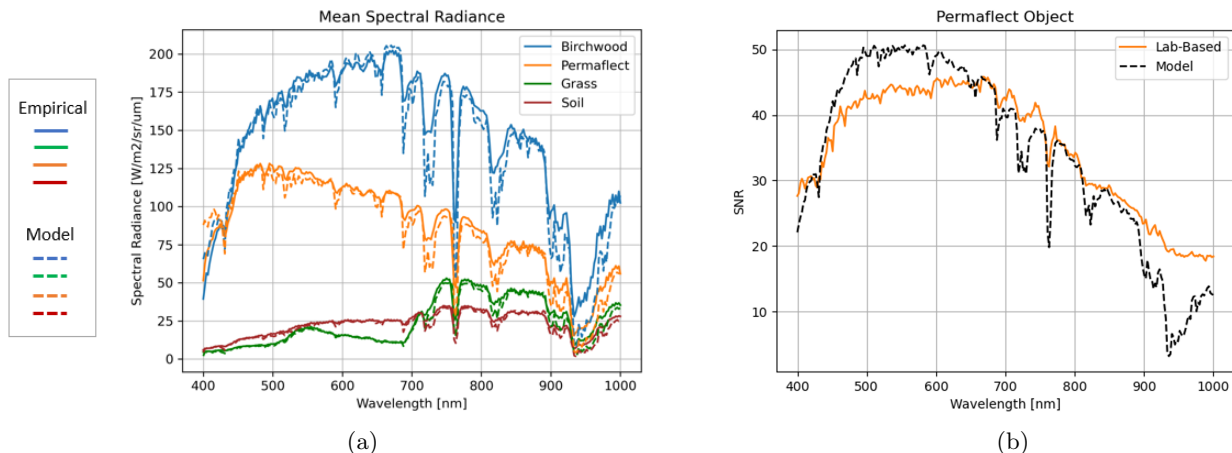


Figure 2: (a) At-sensor spectral radiance validation of target (birchwood) and background (permaflect, grass, soil) classes and (b) SNR validation of permaflect background class.

Atmospheric validation was achieved using the mean spectral radiance of the target (birchwood) and background materials (permaflect, grass, soil); as observed in 2a, good co-agreement was achieved between the empirical and model results. Error in at-sensor radiance can be attributed to inaccuracies in modeling precise atmospheric constituents (water vapor, aerosols, haze) within MODTRAN. Sensor validation was achieved using the signal-to-noise ratio of the permaflect object; as observed in Fig. 2b, acceptable co-agreement was achieved between the empirical and model results. The SNR can be a complex measurement, as shot noise varies with signal strength. Therefore, a psuedo “lab-based” empirical-model of SNR was used in lieu of an empirical measurement. The method involved collecting SNR measurements, as a function digital counts (DC), of a “high” (near saturation) and “low” signal in a laboratory using a QHT illumination source. The 2-point laboratory measurements were then interpolated to generate a lab-based model (SNR versus DC), using methods analogous to the empirical line method (ELM). This technique does assume the detectors respond linearly, which is an over-simplification. Afterwards, empirical measurements of the permaflect material within the raw (DC) UAS image were collected. The lab-based model was then applied to the empirical measurements to generate the SNR result shown in Fig. 2b.

The final stage of model validation is the detection output in the form of receiver operating characteristic (ROC) curves. Detection is impacted by the number of target and background class samples, which are shown in Table 2. Target samples were selected within central regions of the 12" x 12" structures, to avoid non-uniformity mixtures of background material due to the point spread function (PSF) of the imager. A ground truth mask of the associated target samples and guard regions are shown in Fig. 3.

Table 2: Number of target and background samples.

$\%T_{ar}$	$N_{Tar}$	Class <sub>Back</sub>	$N_{Back}$
100	142	Soil	31349
75	15	Grass	30633
50	21	Perm	130
25 (Tri)	17		
25 (Hex)	15		
25 (Sq)	14		

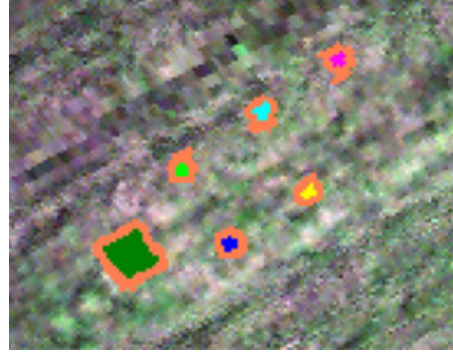


Figure 3: Ground truth mask of real targets.

Empirical ROC curves from the real target samples (i.e. 25%, 50%, 75%, 100%) and the modeled ROC curves of the same target percentages are shown in Fig. 4a. General co-agreement between the model and empirical based results are observed. Specifically, for the 75% and 100% target percentages, “perfect” detection is observed across all false alarms rates, between the model and empirical curves. For the 50% real target, the model and empirical curves align well. Variability across the three 25% real targets is observed with decent model co-agreement.

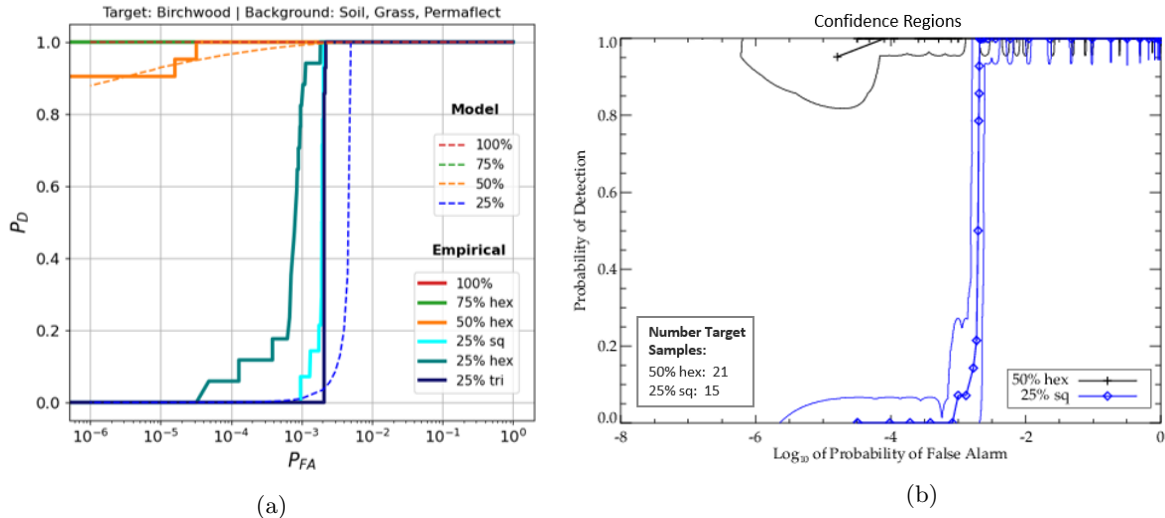


Figure 4: (a) Empirical ROC curves from the various real targets with model ROC curves using the systems parameters in Table 1 and (b) Confidence regions for the 25% sq and 50% hex real targets.

### 3.2 Sources of Error

The three 25% real targets (sq, hex, tri) have been confirmed to have accurate (and equivalent) ground truth target percentages, however, the empirical ROC curves indicate slight differences in detection. Differences can be partially attributed to undersampling, given the limited number of samples across the 25% sq, hex and tri targets were 14, 15, and 17, respectively. Confidence intervals or regions are used to account for random variations of empirical ROC curves.<sup>2</sup> In Fig. 4b, the 95% empirical confidence regions across the 25% sq target implies the



differences between the sq and tri observations are “indistinguishable” if measurements were repeated (i.e. re-sampled) under similar system conditions. The 25% hex target falls outside this confidence region, however, it was discovered other sources of error can explain for this effect. Furthermore, in the model scenario, an infinite number of samples were derived from a population distribution, such that the model ROC curve does not require a confidence region.

Additional sources of error or reasons for variability in the ROC curves can be attributed to material phenomenology effects (i.e. bi-directional reflectance distribution or BRDF), in relation to the sensor-sun geometry.<sup>3</sup> During data collection, many of the targets were unintentionally tilted at various angles on the ground surface. Initially this was not ideal, however, it later presented an interesting case study on the impacts of the material BRDF on detection. Using ground truth images captured with a handheld camera on the day of the data collection, estimations of the target tilt were assessed. Laboratory BRDF measurements were then collected using the goniometer at RIT (GRIT-T) on the birchwood material at various illumination, view zenith, and target rotation angles. It was discovered the differences in detection between the 25% (sq, hex, tri) targets can indeed be attributed to BRDF effects (grain direction of the wood and target tilt). This confirms the differences between the model and empirical validation can be accounted to BRDF effects not considered in the model.

## 4. CONCLUSION

A hyperspectral systems model for subpixel target detection was validated using empirical data from a UAS October 2021 collect at a new location in Rochester, NY. Novel Targets with constant target percentages were designed, fabricated, and deployed for initial conceptual testing to assist in model validation and preliminary exploration of fundamental limits of subpixel detection. Model parameters, including elements of the scene, sensor, atmosphere and processing were defined using parameters characterized from the empirical data. The case study included subpixel targets of birchwood mixed onto a soil background, and a scene consisting of soil, grass and permaflect background classes. The atmosphere and sensor stages of the model were validated using empirical measurements of the at-sensor radiance and signal-to-noise ratio. The final stage of validation (i.e. detection) was validated using receiver operating characteristic (ROC) curves. The systems model revealed good co-agreement between the empirical results, with variability attributed to undersampling the real targets (confidence regions) and material phenomenology effects (BRDF).

A new model reconfiguration of the hyperspectral systems model is currently under development. Validation efforts were important for establishing baseline functionality and exploring sources of model uncertainty using real data. After validation, the utility of the model will be leveraged to investigate fundamental limits of detection in subpixel objects, through parametric trade studies. One example is detection versus target percentage. This will be investigated further in the near future using the re-designed hyperspectral model and re-defined novel targets in upcoming experiments.

## ACKNOWLEDGMENTS

This work was supported in part by NGA University Initiative grant HM04762110005. The authors thank Dave Conran (RIT) for collecting SNR laboratory measurements of the Headwall Nano sensor. The authors thank Chris Lee (RIT) and Nayma Nur (RIT) for collecting the BRDF laboratory measurements. The authors thank Nina Raqueno (RIT) and Timothy Bauch (RIT) for their assistance collecting the UAS data.

## REFERENCES

- [1] Kerekes, J. and Baum, J., “Spectral imaging system analytical model for subpixel object detection,” *IEEE Transactions on Geoscience and Remote Sensing* **40**, 1088–1101 (May 2002).
- [2] Kerekes, J., “Receiver Operating Characteristic Curve Confidence Intervals and Regions,” *IEEE Geoscience and Remote Sensing Letters* **5**, 251–255 (Apr. 2008). Conference Name: IEEE Geoscience and Remote Sensing Letters.
- [3] Ientilucci, E. J., “Oblique hyperspectral radiometric phenomenology study,” in [*Image and Signal Processing for Remote Sensing XV*], **7477**, 209–220, SPIE (Sept. 2009).